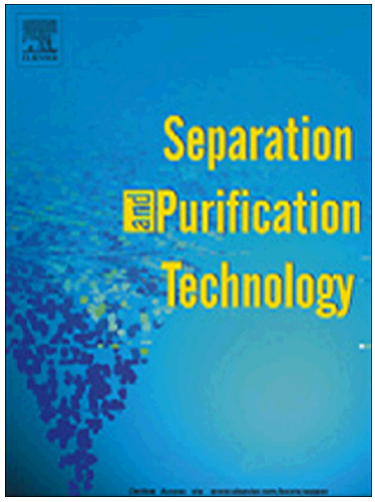

Electrochemical treatment of wastewater from almond industry using dsa-type anodes: direct connection to a pv generator

David Valero, Vicente García-García, Eduardo Expósito, Antonio Aldaz, Vicente Montiel

PII: S1383-5866(13)00723-5
DOI: http://dx.doi.org/10.1016/j.seppur.2013.12.023
Reference: SEPPUR 11542

To appear in: *Separation and Purification Technology*

Received Date: 18 September 2013
Revised Date: 16 December 2013
Accepted Date: 24 December 2013

Please cite this article as: D. Valero, V. García-García, E. Expósito, A. Aldaz, V. Montiel, Electrochemical treatment of wastewater from almond industry using dsa-type anodes: direct connection to a pv generator, *Separation and Purification Technology* (2013), doi: http://dx.doi.org/10.1016/j.seppur.2013.12.023

ELECTROCHEMICAL TREATMENT OF WASTEWATER FROM ALMOND INDUSTRY USING DSA-TYPE ANODES: DIRECT CONNECTION TO A PV GENERATOR

David Valero, Vicente García-García, Eduardo Expósito*, Antonio Aldaz, Vicente Montiel

Grupo de Electroquímica Aplicada, Instituto Universitario de Electroquímica, Departamento de Química Física, Universidad de Alicante, Apdo. 99, Alicante, 03080, Spain

*Corresponding author: Dr. Eduardo Expósito, email: eduardo.exposito@ua.es, Address: Instituto Universitario de Electroquímica, Universidad de Alicante, Apdo. 99, Alicante, 03080, Spain. Telf.: +34965903628, Fax: +34965903537.

ABSTRACT

Food industries such as almond industry generate large volumes of wastewater in their processes and common techniques are not always efficient for treating this kind of effluents. In this work, the feasibility of a treatment for pollutants removal of a real industrial wastewater by electrochemical oxidation s studied at laboratory scale and then scaled-up to pre-industrial scale. The first stage of the work was performed at laboratory scale, using a 63 cm^2 cell, where different anodes (Ti/Pt, and DSA anodes (Ti/RuO_2 and Ti/IrO_2)) and the optimal experimental conditions (pH, current density, temperature and [Cl^-]) were studied and established. By using a DSA-Cl_2 anode (Ti/RuO_2), pH 9, j = 50

mA cm^{-2}, [Cl^-] = 2000 mg L^{-1} and room temperature, chemical oxygen demand (COD) was removed up to 75 % and results show that electrooxidation can remove organic pollutants.

In the second stage the scaling-up of the process from laboratory to pre-industrial scale was performed, by using a 3300cm^2 cell. The electrochemical reactor was finally powered by a photovoltaic generator directly connected, in order to operate by using a renewable energy and a COD elimination of 80 % was achieved.

KEYWORDS

Electrochemical oxidation

Industrial wastewater

Photovoltaic energy

Pre-industrial scale

1. INTRODUCTION

Almond industry is an important market segment in food industry and Spain is the second producing country in the world with the 11 % of total almond production [1]. The industrial processing of almonds includes several steps, including cracking and blanching. The organic content of the wastewater from the blanching step is high and, for this reason, the wastewater must be treated before its reuse or discharge to sewage systems. Moreover, almond industry is seasonal, working mainly during the harvest time and that is why the wastewater treatment facilities must cope with a huge amount of wastewater during short periods of time. Wastewater from almond industry has high

values of suspended solids (SS), total organic carbon (TOC), chemical oxygen demand (COD), turbidity and colour.

Among the different techniques for wastewater treatment, electrochemical methods have achieved a relevant position [2-11] and the most applied technologies are the oxidation of organic pollutants by cathodic generation of hydrogen peroxide [12-14], the anodic oxidation using different electrodes [15-17], the cathodic removal of metals [18] and the electrocoagulation [19-23].

Electrocoagulation (EC) has shown to be a suitable method for reducing pollutants from almond industry wastewater, as it was reported in a previous work where EC reduced up to 99 % of SS, turbidity and colour, and 80 % of COT and COD from it [20]. However, although EC is a suitable technique to eliminate suspended solids and particles able to flocculate, it is not appropriate when soluble organic matter is the main pollutant to be removed. When the treated wastewater is directly discharged to the sewage system, it must satisfy the discharge limits established by existing legislation. Spanish discharge limits are 1000 mg L^{-1} for COD and 500 mg L^{-1} for SS [24, 25]. In addition, if the wastewater is to be reused, limits are lower and COD must be more deeply reduced [26]. So, in those cases where EC is not able to reduce COD under discharge limits, it is compulsory to use an additional treatment before the wastewater is discharged.

Electrooxidation (EO) has shown to be an effective method for reducing pollutant load from water containing soluble organic matter and numerous studies where EO is applied for treating different pollutants, such as phenol, have been published [17, 27-28]. On the other hand, EO systems are not designed for treating water containing high amounts of

suspended solids. Therefore, wastewater containing suspended solids should be firstly treated, for example by EC, to remove those solids before sending the wastewater to an EO treatment system.

The oxidation of the organic compounds in the solution can follow two different paths: direct and indirect oxidation. When chloride anions are present in the solution, the main path is the indirect oxidation by means of the different electrogenerated species (eq. 1-3), the nature of which depends on the pH. In this case we will work under alkaline conditions, where hypochlorite is the main active agent for the oxidation [29, 30]. Working under alkaline conditions minimizes the possibility of formation of toxic halocompounds and organochloride species, as it has been described by some authors [17, 31].

$$2Cl^- \rightarrow Cl_2 + 2e \quad (1)$$

$$Cl_2 + H_2O \rightarrow HClO + H^+ + Cl^- \quad (2)$$

$$HClO \leftrightarrow H^+ + ClO^- \quad (3)$$

Moreover, it is important to highlight that electrochemical reactors operate with dc current, which can be supplied by a renewable energy source, such as photovoltaic cells (PV). Direct coupling of electrochemical reactors and PV cells have been successfully tested in previous works [22, 32-36], where it was demonstrated that i) the use of the PV energy decreases the investment cost by avoiding the use of batteries, solar inverters and power supplies and ii) maintenance cost decreases, since there is no battery waste to manage.

Therefore, the aims of this work are to demonstrate that electrooxidation, when applied after electrocoagulation, is a suitable technology for the treatment of wastewater generated by the almond industry; to study the influence of experimental conditions of the EO process on the removal of pollutants at laboratory scale; to perform the scaling-up to a pre-industrial scale by applying the optimal conditions found at laboratory scale; and finally, to demonstrate the feasibility of an EO process directly powered by a PV generator (EO-PV).

2. EXPERIMENTAL

2.1 Laboratory-scale.

2.1.1. Wastewater description.

The wastewater samples used came from an industry located in the southeast of Spain and were taken from a homogenization tank placed after the blanching process. The colour of these murky wastewaters was brown and contained a large amount of suspended solids and a high COD value. Since the pollutant concentration in the wastewater may vary depending on the daily activity of the industry, the samples used in the laboratory study and in the pre-industrial scale–up study were slightly different.

As we have mentioned before, suspended solids might be a problem for the electrooxidation system, so, the first step was to use an electrocoagulation treatment to decrease the amount of SS. The experimental laboratory system for the electrocoagulation of this wastewater is explained in a previous work [20], where the experimental conditions are also described: no pH adjustment (initial value is 5.7), current density (j) 5 mA cm^{-2}, time of treatment 15 minutes, aluminium anode and iron

cathode. Table 1 shows the analytical parameters of the wastewater after the EC treatment, which are the initial analytical parameters for the EO process.

	Initial Laboratory EO water	Initial Pre-Industrial EO water
pH	6.2	6.7
Conductivity (mS cm^{-1})	2.2 (23 ºC)	5.3 (21 ºC)
TOC (mg L^{-1})	710	410
COD (mg L^{-1})	2000	1300
Total Nitrogen (mg L^{-1})	23	14
Phosphorus (mg L^{-1})	0.07	0.2
Apparent colour (Pt/Co units)	310	249
Suspended solids (mg L^{-1})	55	33
Turbidity (FTU units)	58	47
Chloride (mg L^{-1})	400	2000

Table 1. Analytical parameters for the wastewater in laboratory and pre-industrial scale.

2.1.2. Experimental system.

The experiments were carried out in batch mode of operation. Wastewater was pumped to the electrochemical reactor using a circulating pump Sanso PMD-311. Temperature and pH were measured by a Mettler-Toledo SevenEasy pH-meter with temperature probe, inserted after the reactor. A Selecta Frigiterm thermostated bath was used for temperature control, whereas conductivity was measured by using a Crison Instruments 525 conductimeter.

The electrochemical reactor used was a non-divided electrochemical filter press reactor, as shown in figure 1.a. As cathode, a stainless steel electrode was used, whereas several materials were tested as anodes: a DSA-Cl_2 (Ti/RuO_2), a DSA-O_2 (Ti/IrO_2) and a Ti-Pt electrode, all of them in the form of a mesh and supplied by ID Electroquímica. The electrode geometric area was 63 cm^2. The electrochemical reactor was powered by a

Horizon Electronics 28V-15A DC power source. Current intensity and reactor voltage were measured using Fluke 179 multi-meters. In addition, the total charge passed was measured by a Digatron AHC1 coulomb meter.

The solution volume was 0.8 L for every experiment and the chloride concentration, when needed, was adjusted by adding the required amount of NaCl Panreac QP. After adjusting the initial chloride concentration $[Cl^-]^o$, the pH was set by adding Na_2CO_3 Panreac PRS directly to the tank.

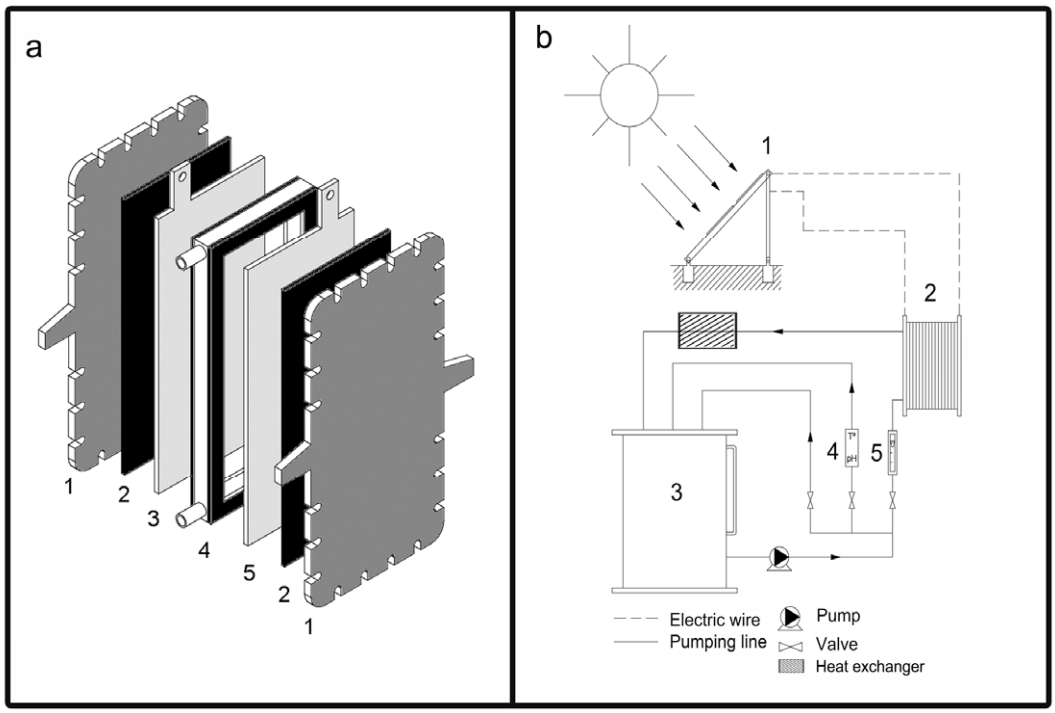

Figure 1. (a) Scheme of the electrochemical reactor: 1. End plates; 2. Insulator gaskets; 3. Cathode; 4. Compartment frame; 5. Anode. **(b)** Diagram of the Pre-industrial system. 1. Solar Photovoltaic generator; 2. Electrochemical reactor; 3. Solution tank; 4. Thermometer and pH-meter; 5. Flow rate meter.

2.2 Pre-industrial scale.

2.2.1. Wastewater description.

For this part of the work, a new wastewater sample was taken from the homogenization tank. As previously mentioned in section 2.1.1, the composition of this sample was different from the sample used for the laboratory study. An electrocoagulation process was applied to the sample by using the pre-industrial system described in a previous work [20] and under the same conditions as in the laboratory scale, in order to reduce suspended solids and other parameters. The chloride concentration was set to 2000 mg L^{-1} by adding NaCl to reproduce the optimal conditions for EO. The sample obtained was used as the initial sample for the electrooxidation process and its composition is showed in table 1. COD values are lower than in the laboratory-scale process, but it is high enough to carry out the electrooxidation process.

2.2.2. Experimental system.

For every experiment in this section, a volume of 20 L of wastewater was used, [Cl^-] was adjusted to 2000 mg L^{-1}, flow rate was 450 L h^{-1}, initial pH was adjusted to 9 by adding Na_2CO_3 and treatment time was 5.5 h. Samples were taken and COD was analyzed. The experimental system consisted of an electrochemical reactor, a 100 liter tank for the solution, pumps, heat exchanger, flow meters and either 80 PV cells or a conventional power supply as power source. The experiments were carried out in a batch mode of operation. Figure 1.b. shows a scheme of the EO-PV system. The electrochemical reactor was a non-divided filter-press reactor, with a DSA-Cl_2 anode made of an active coating of ruthenium oxide (RuO_2) deposited on a titanium mesh, whereas the cathode was a stainless steel mesh. The geometric area per electrode was 3300 cm^2 and the temperature was controlled by using a heat exchanger.

A Quasar Q500 250A-10 V was used as the electric power source. The photovoltaic cells employed were made of polycrystalline silicon, PQ10/40/01-02 (AEG), with a peak power of 38.48 W per cell, an open circuit voltage of 20 V, and an area of 0.5 m^2 (1 m × 0.5 m) each. The experiments were carried out at the University of Alicante (latitude 38°24′05″ N, longitude 0°31′ W, altitude 109 m above sea level). The tilt of the photovoltaic cells was 55° and the PV array was south-facing (0.4° W). The PV array consisted of 80 cells connected in parallel. The incident solar radiation was measured using a pyranometer 80 SPC (Soldata Instruments). Electric parameters such as cell voltage, PV voltage, current intensity, irradiation and charge were registered using a data acquisition system connected to a computer.

2.3 Analytical Methods.

The efficiency of the electrochemical oxidation process was measured by following the change of COD values during the experiments. Total organic carbon (TOC) and total nitrogen were measured with a SHIMADZU TOC-V Total-N CSH analyzer. COD and the rest of analytical parameters were measured by a HACH DR 2000 spectrophotometer.

3. RESULTS AND DISCUSSION

3.1. Laboratory scale. Study of the experimental conditions.

- **Influence of anode material**

The anode material is a factor that strongly influences the efficiency of electrooxidation processes and for this reason, it was the first parameter studied in this work. In the last decades, several electrodes, such as Pt, DSA-Cl_2, DSA-O_2, Ti/SnO_2, Ti/PbO_2, Ti/Pt and BDD, have been evaluated as anodes in terms of activity towards direct or indirect

electrooxidation, stability, cost and reliability. These electrodes have different oxidation power [27, 37-40] and some of them, such as BDD are, by now and in spite of its higher oxidation efficiency, too expensive to be used in industrial processes.

In this work, Ti/Pt, DSA-Cl_2 and DSA-O_2 anodes were selected to be evaluated due to both, i) their relatively moderate cost and reliability at industrial scale and ii) they have been commonly used for wastewater treatment [41-44]. Each electrode needs some experimental conditions recommended by the manufacturer, for example, for DSA-Cl_2 pH has to be between 9 and 11 and the maximum chloride concentration should be 5000 mg L^{-1}. On the other hand, for DSA-O_2 pH has to be under 8, maximum j should be 150 mA cm^{-2} and only chloride traces are allowed.

The experiments in this section were all carried out using 0.8 L of wastewater, current density was 25 mA cm^{-2} and temperature was set at 25ºC. Because of the above-mentioned experimental requirements for each electrode, pH and chloride concentration were slightly different. For the experiment with the DSA-Cl_2 electrode, chloride concentration was adjusted to 5000 mg L^{-1} by addition of NaCl and pH was adjusted to 10 by adding Na_2CO_3. For the experiments with the DSA-O_2 and Ti/Pt electrodes, no chemicals were added. In these cases, pH was 6.7 and conductivity was 2 mS cm^{-1}.

COD removal rates (% COD/CODº) vs. time results are shown in Figure 2.a. The figure shows that DSA-O_2 and Ti-Pt electrodes achieved a low COD removal rate. On the other hand, DSA-Cl_2 electrode achieved a higher COD removal rate and for this reason, the electrode used for the rest of the work was the DSA-Cl_2 electrode.

- **Influence of pH**

In order to determine the optimum pH value for the electrooxidation treatment, a series of experiments in the pH interval 9-11, which is recommended by the manufacturer, was carried out. Considering that pH was decreasing during the experiments, Na_2CO_3 was continuously added to the tank in order to keep a constant value. Figure 2.b shows that the higher COD removal was found at pH 9. Furthermore, carrying out the experiments at pH 9 requires lower amounts of chemicals for adjusting pH (0.62 g $Na_2CO_3\,L^{-1}$) and in addition, it satisfies the discharge limit for pH.

- **Influence of j**

Current density is one of the most important parameters in electrochemical processes. An optimum value of j allows us to control the electrochemical process, to avoid undesired parallel reactions, to improve current efficiency and to reduce the energy costs. To this end, a series of experiments at several values of j were carried out.

Figure 2.c. (COD vs. Passed Charge) shows that the current efficiency is similar for all the experiments, i.e. the charge needed for decreasing COD to 1000 mg L^{-1} is similar for different current densities. However, as it can be seen in figure 2.d., the curve COD vs. time shows that the time needed to achieve the limit COD value raises dramatically when j decreases. When j is 25 mA cm^{-2} treatment time needed to get 1000 mg L^{-1} was 4.5 h, whereas 2.3 h and 1.8 h were needed when j is 50 and 75 mA cm^{-2} respectively. COD removal rates and other parameters when j is 50 and 75 mA cm^{-2} are similar. The main difference between them is the higher energy consumption when j increases. Cell voltages are 4.5 and 4.9 V respectively. The chosen j value is 50 mA cm^{-2}, in order to

get a high performance at short treatment time and low value of energy consumption. Furthermore, this j value will be reproducible at the pre-industrial scale system.

- **Influence of Temperature**

Another pattern studied was the influence of temperature in the process; therefore three experiments were performed at 15, 25, 40 ºC respectively. Moreover, a last experiment under uncontrolled temperature conditions was also made, where the temperature increased from an initial value of 19 ºC up to 36 ºC. Figure 2.e. shows that temperature has little influence on COD removal. In fact, the last experiment where temperature is not controlled achieves similar elimination than experiments with controlled and constant temperature.

- **Influence of [Cl^-]**

Next, the minimum amount of chloride salts to be added to the solution will be established. [Cl^-] must be enough to form the necessary amount of oxidizing species and to supply conductivity in order to decrease the cell voltage. However, the amount of added chloride should not be excessive because the conductivity parameter for water disposal is controlled by law–discharge limit is 3 mS cm^{-1}– and chemicals consumption must be minimized. With that aim, a series of experiments at different [Cl^-] were performed.

Results are shown in figure 2.f. where it can be seen that, in a general way, the higher [Cl^-], the better COD removal. When [Cl^-] is 3000 mg L^{-1} or higher, better removal rates are achieved, but conductivity gets values higher than 9 mS cm^{-1}, which are very far from the discharge limit. In this point, two options must be considered: 1. Setting a low

[Cl^-] to have a conductivity value according to the law, but it increases treatment time needed for decreasing COD to the discharge limiting value; 2. Setting a higher [Cl^-] to decrease treatment time, cell voltage and energy consumption but in this case, discharge limit is not satisfied and a further treatment for decreasing conductivity is needed, increasing the cost of the treatment. The choice among these options will depend on the nature and the purpose of the water to be treated (discharging to sewage system, reuse, etc); therefore, cost estimation must be done.

Table 2 shows initial and final conductivity and cell-voltage values for every [Cl^-]. By using these parameters, an estimation of energy consumption has been made taking into account the time needed to achieve 1000 mg L^{-1} of COD (equation 4). As expected, the higher [Cl^-], the lower energy consumption.

In this case, the optimal value of [Cl^-] is 2000 mg L^{-1}, a compromise value that counterbalances final conductivity, energy consumption and treatment time.

$$\text{Energy consumption (kW h m}^{-3}) = \frac{\text{Intensity (A)} \cdot \text{Cell voltage (V)} \cdot \text{time (h)}}{\text{Volume (L)}} \quad (4)$$

[Cl^-] (mg L^{-1})	Initial Cond. (mS cm^{-1})	Final Cond. (mS cm^{-1})	Voltage (V)	Time for COD 1000 mg L^{-1} (h)	Energy consumption (kW h m^{-3})
400	2.6	3.4	6.7	>15	>400
700	3.0	3.3	6.3	9.1	226
1000	4.5	5.3	5.6	5.1	112
2000	7.0	7.1	5.1	4.4	88
3000	9.1	9.1	4.8	2.6	49
4000	13.3	12.9	4.4	2.2	38

Table 2. Experimental data, including time needed to reduce COD to 1000 mg L^{-1} and energy consumption to achieve this value, for experiments at laboratory scale.

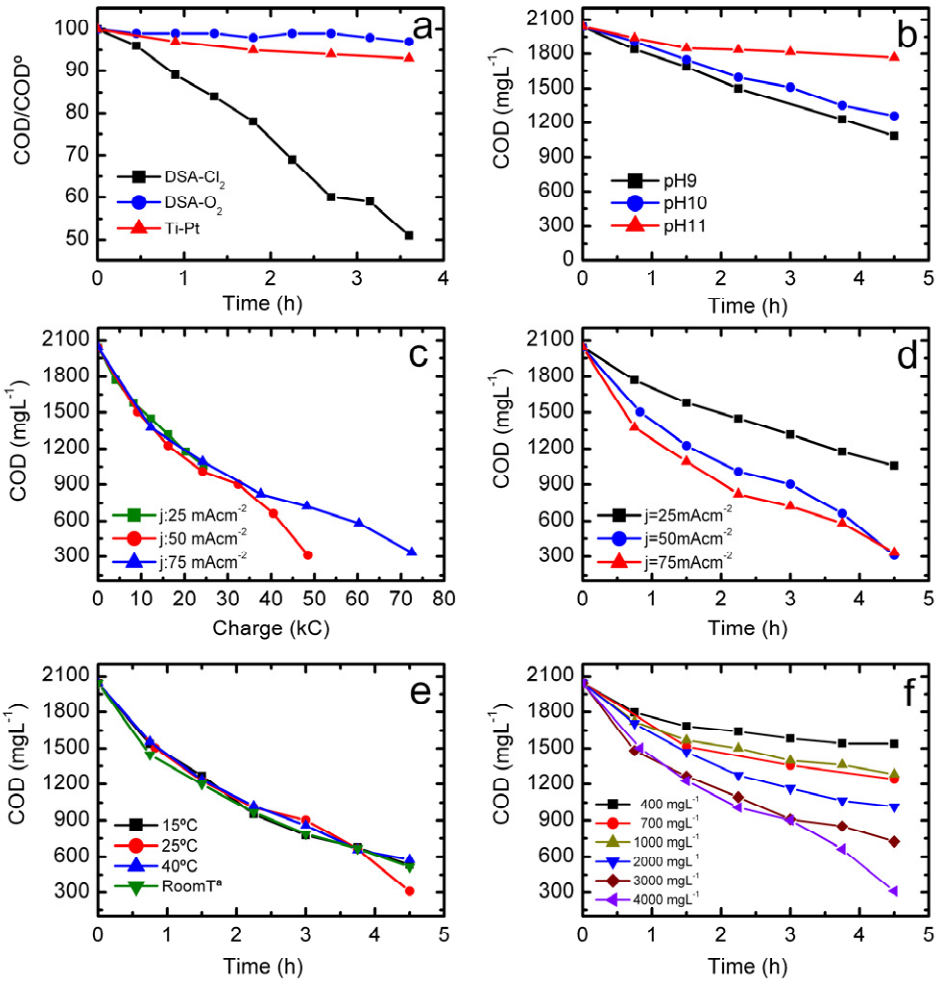

Figure 2. a) Percentage of remaining COD vs. time for different electrodes. **b)** COD vs. time for different pH. [Cl^-]: 5000 mg L^{-1}, 25 ºC, j: 25 mA cm^{-2}. **c)** COD vs. passed charge for different current densities (j). [Cl^-]: 3000 mg L^{-1}, 25 ºC, pH 9. **d)** COD vs. time for different current densities. [Cl^-]: 3000 mg L^{-1}, 25 ºC, pH 9; **e)** COD vs. time for different temperatures. [Cl^-]: 3000 mg L^{-1}, pH 9, j: 50 mA cm^{-2}; **f)** COD vs. time for different chloride concentrations. 25 ºC, pH 9, j: 50 mA cm^{-2}.

3.2. Pre-industrial scale.

Once the optimal experimental conditions had been established -in previous section- to carry out the electrooxidation treatment of this wastewater, the scaling-up of the

electrooxidation process to a pre-industrial size was performed and meanwhile, the feasibility of the coupled system EO-PV was demonstrated and its behaviour was explained. With this aim, in order to know the operating values of the electrical parameters (Vcell, I) in this reactor powered by a conventional power source and to perform the scaling-up, a first experiment was carried out. Once these values were known, we selected the configuration of the cells and finally two experiments powered by the photovoltaic cells at different weather conditions were performed.

3.2.1. Conventional power source.

A first experiment powered by the conventional power source (Exp. 1) was carried out in order to study the behaviour of the system. This experiment was performed at a constant voltage value of 10V, therefore the changes in the intensity (85 −125A) were due to the variations of the temperature (18 –32ºC) of the solution. Figure 3.a. shows the curves intensity and voltage vs. time for Exp. 1. Under these conditions, it was possible to carry out the reaction and reduce COD levels of the wastewater in an extension that is enough to characterize the system. COD vs. time curve is shown in Figure 3.b. (Exp. 1). As it can be seen, the shape of the curve of COD removal at pre-industrial scale was similar to the curves obtained at laboratory scale and the removal rate also reached similar values.

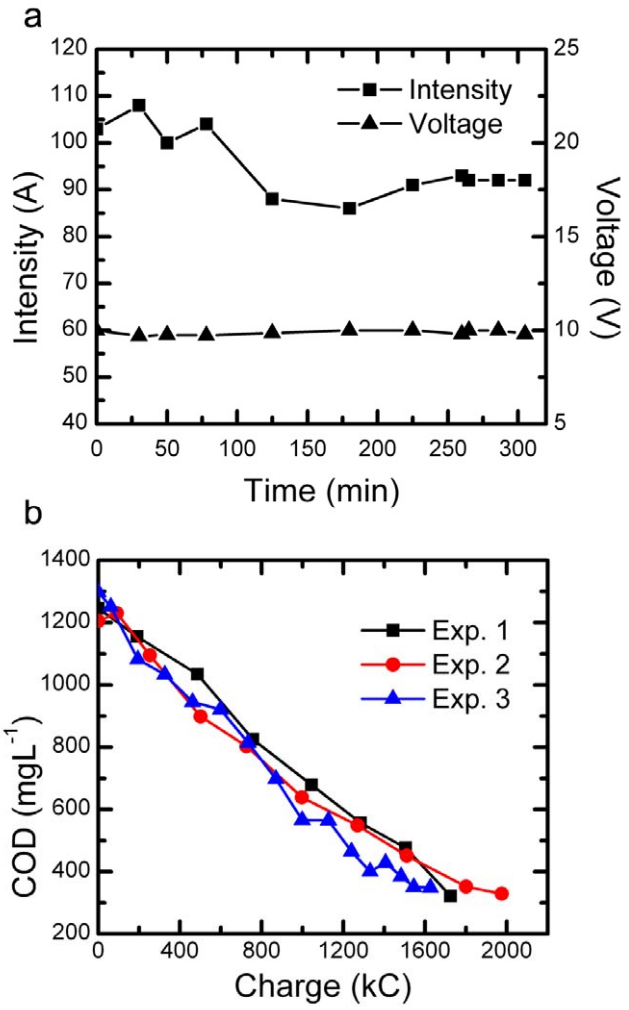

Figure 3. (a) Current intensity and voltage vs. time for Experiment 1. **(b)** COD variation vs. passed charge for pre-industrial scale experiments.

3.2.2. PV generator.

In order to compare the results obtained by powering the system with the conventional power source and the PV generator, the configuration of the generator was set to provide similar values of the electrical parameters to those applied in Exp. 1. To this aim, it is necessary to choose the size and configuration of the PV generator to give similar values to the maximum intensity supplied by the Quasar source. An optimal configuration of the PV generator means to know how these systems work [45]. The

behaviour of the photovoltaic-electrochemical systems was described in a previous work [33].

It should be interesting to briefly indicate the most important parameters of the characteristic I-V curve of the PV cells, with the purpose of understanding the experimental behaviour of the coupled EO-PV system. Figure 4.a. shows the I-V curve for a single PV cell and for a given irradiation, temperature and load. The shaded area is the power delivered by the cell for different external loads.

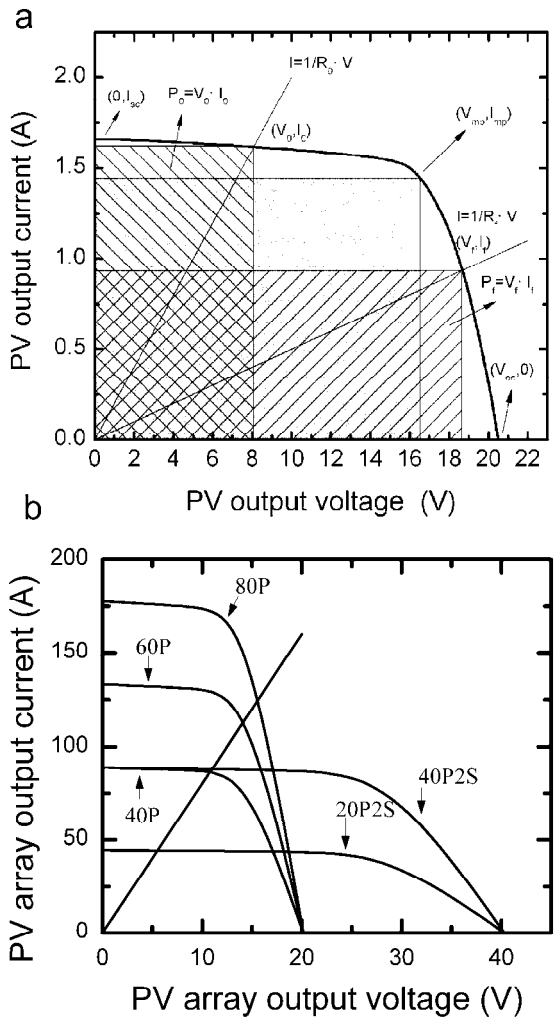

Figure 4. Characteristic curve at G= 800 W m^{-2} and T_{cell}=298 K of: **a)** a single PV cell; **b)** array of cells.

The parameters that define a PV cell are the short-circuit current (I_{sc}) and the open-circuit voltage (V_{oc}). I_{sc} is the current given by the PV cell when the voltage between terminals is zero (R_{load}=0). V_{oc} is the voltage measured in absence of connected load (or R_{load}=•). The maximum power (P_m) is the electrical maximum power that a PV cell can give for a given solar irradiation (G) and cell temperature (T_{cell}). It is defined by the point of the I-V curve where the product of the current (I_{mp}) and voltage (V_{mp}) is maximum.

Figure 4.a. shows two clearly differentiated zones. Firstly, a plateau is observed where the values of current are approximately equal to I_{sc} for a wide range of voltages. The second region is characterized by a sudden decrease of the current, being the voltage approximately equal to V_{oc}. Figure 4.a. also shows that for a load with an electrical resistance R_0, the intersection of the characteristic I-V curve of the PV cell with the straight line $I=(1/R_0)V$ defines the working point of the cell.

PV cells can be connected in series or in parallel. If a group of identical PV cells are connected in series forming a PV array, the open circuit voltage ($V_{oc,array}$) of the array increases with the number of cells connected in series (n) -approximately $V_{oc,array} = nV_{oc}$. However, the short circuit current ($I_{sc,array}$) remains approximately equal to the value of a single PV cell, I_{sc}. Similarly, when a group of identical PV cells are connected in parallel, $I_{sc,array}$ increases with the number of cells connected in parallel (m) -approximately $I_{sc,array} = mI_{sc}$, and $V_{oc,array}$ is the same as the one with a single PV cell, V_{oc}.

At this point, we needed to choose the configuration of the PV generator. Our solar plant consists of arrays of 20 cells connected in parallel (20P), which we can connect in series or in parallel, i.e. 2, 3 or 4 of these stacks connected in parallel (40P, 60P and 80P

respectively) or combinations such as 2 stacks connected in series (20P2S) or 2 stacks connected in parallel and two of these 40P connected in series (40P2S). Fig. 4.b. shows the theoretical curves for the mentioned configurations for a given irradiation and an external load equivalent to the internal resistance of the electrochemical reactor working with a sample with the conductivity and the temperature of the working solution. It can be seen that the configuration of the PV generator consisting of 80 cells connected in parallel (80P) supplies the maximum power and current intensity, which allows reproducing the electric conditions of Exp. 1. For this reason, this was the chosen configuration of the generator for all the experiments in this section.

Experiments nº 2 and 3 were powered by the PV generator, at different weather conditions (Fig. 5). Experiment nº 2 took place in a sunny day and the Irradiation vs. time curve has the typical hill-shape, as shown in figure 5.a., whereas different regions with different slopes can be seen at the Intensity vs. time curve. The first one, until t=50 min., represents the first moments of the day when the cells are partially in the shade and they are not able to provide the maximum power. When the shadow finishes, the slope of the curve changes and the intensity raises faster for the same increment of Irradiation. At t=75 min, Intensity achieves its maximum value and it remains constant despite Irradiation is still raising. At the end of the day the curve shows the reverse behaviour. The curves in Fig. 5.c. correspond to the characteristic curves of the PV generator at points A, B and C in Fig. 5.a. As it can be seen in Fig. 5.c., the working points for the three chosen moments are located at the region of the *I-V* curve characterized by a fast decrease of the current intensity, not in the plateau. When irradiation rises, the plateau of the curve and the I_{sc} value also rise but it does not affect the current intensity of our system because the second region of the curve does not change. So, when the working point is located in this region, an increase in the

irradiation does not mean an increase in intensity. For this reason, points B and C show the same Intensity value despite the Irradiation at point C is higher than at point B.

On the other hand, experiment nº 3 was performed in a day with cloudy intervals (Fig. 5.b). Along this experiment irradiation fluctuates and intensity varies according to it, as it can be seen at the region around point D. Under these conditions, intensity also achieves a maximum value (point E) but when irradiation dramatically decreases, intensity diminishes proportionally (point F).

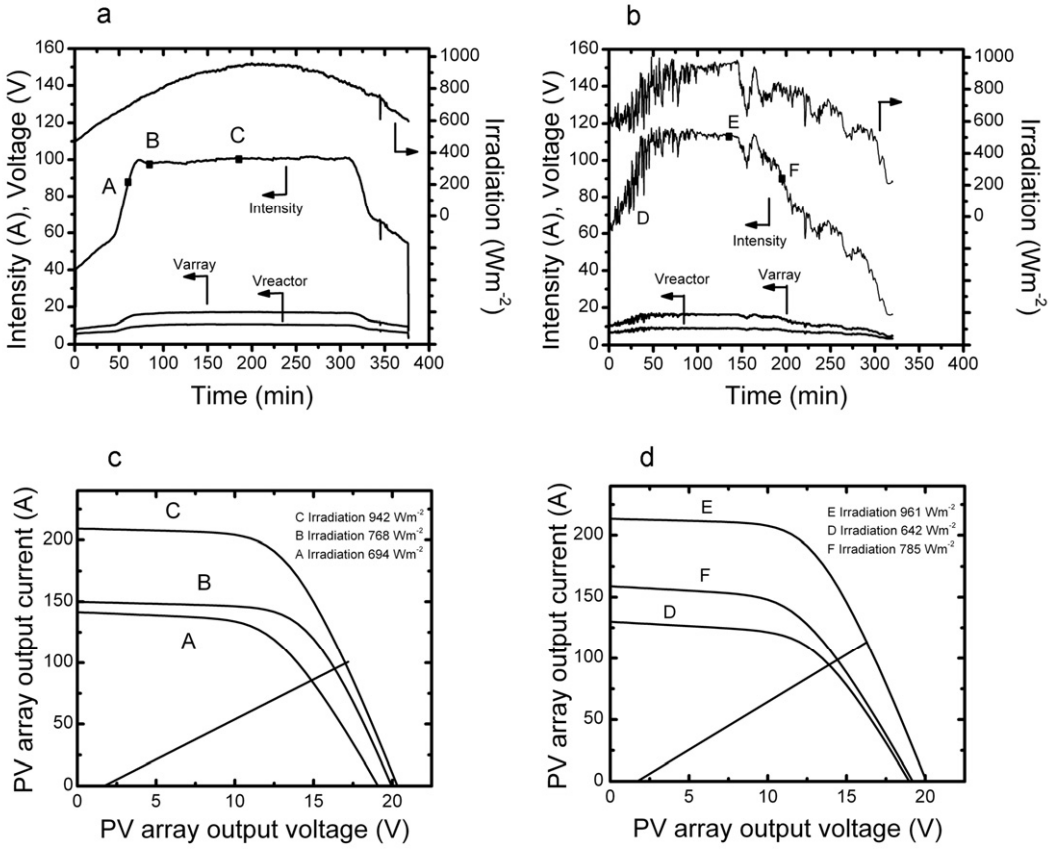

Figure 5. a) Curves of Intensity (A), Vreactor (V), Varray (V) and Irradiation (W m^{-2}) vs. time for Experiment 2, marking three different working points: A, B and C. **b)** Characteristic I-V curve of the PV generator for points A, B, and C in Experiment 2. **c)** Curves of Intensity (A), Vreactor (V), Varray (V)

and Irradiation (W m^{-2}) vs. time for Experiment 3, marking three different working points: D, E and F. **d)** Characteristic I-V curve of the PV generator for points D, E, and F in Experiment 3.

Figure 3.b shows the variation of COD vs. electrical charge for these experiments. The COD removal rate is very similar, and at the end of the experiments a COD value of 350 mg L^{-1} is reached, which represents a 70% of removal. Moreover, it can be seen that there is no influence of the type of power source or the weather conditions on the removal rates, which proves the operational stability and reliability of the pre-industrial electrooxidation system. The stability of the process is probably due to the fact that the oxidation of the organic matter follows an indirect path by means of hypochlorite, and this way of oxidation does not directly depend on the electric supply of the reactor and electrogenerated species go on with the reaction despite irradiation has fluctuations. The analytical parameters of the treated wastewater are shown in table 3.

	Treated wastewater
pH	6.7
Conductivity (mS cm^{-1})	7.2
TOC (mg L^{-1})	296
COD (mg L^{-1})	350
Total Nitrogen (mg L^{-1})	11.3
Phosphorus (mg L^{-1})	0.24
Apparent colour (Pt/Co units)	34
Suspended solids (mg L^{-1})	5
Turbidity (FTU units)	6
Chloride (mg L^{-1})	900

Table 3. Analytical parameters of wastewater after electrooxidation treatment at pre-industrial scale.

Because of the addition of Cl^- to enhance the EO treatment, the conductivity might increase. In the event that treated wastewater has high conductivity, a post-treatment

might be necessary in order to reduce it. This post-treatment is the aim of a forthcoming research.

4. CONCLUSIONS

In this work, the variables that affect the electrooxidation process applied to an almond industry wastewater – pre-treated by an electrocoagulation process– have been studied at laboratory scale: anode material, pH, current density, chloride concentration and temperature. The optimal conditions found for the treatment were: a DSA-Cl_2 anode, pH 9, j = 50 mA cm^{-2}, $[Cl^-]$ = 2000 mg L^{-1} at room temperature. COD elimination rate under these conditions was 75% so, it has been demonstrated that electrooxidation is a suitable technique for the treatment of wastewater from almond industry.

A pre-industrial electrooxidation system, powered by PV energy, was built and tested. COD elimination rate achieved 70 % and it was reduced under discharge limit established by existing legislation, when treating wastewater by this pre-industrial system. So, the feasibility of these systems has been proved.

REFERENCES

[1] Food and Agriculture Organization of the United Nations, FAOSTAT, 2011.

[2] I. Sirés, E. Brillas, Remediation of water pollution caused by pharmaceutical residues based on electrochemical separation and degradation technologies: A review, Environ. Inter. 40 (2012) 212-229.

[3] A.T. Yeunga, Y. Gub, A review on techniques to enhance electrochemical remediation of contaminated soils, J. Hazard. Mater. 195 (2011) 11-29.

[4] M.A. Rodrigo, P. Cañizares, C. Buitrón, C. Sáez, Electrochemical technologies for the regeneration of urban wastewaters, Electrochim. Acta 55 (2010) 8160-8164.

[5] A. Anglada, A. Urtiaga, I. Ortiz, Contributions of electrochemical oxidation to waste-water treatment: fundamentals and review of applications, J. Chem. Technol. Biotechnol. 84 (2009) 1747–1755.

[6] C.A. Martínez-Huitle, E. Brillas, Decontamination of wastewaters containing synthetic organic dyes by electrochemical methods: A general review, Appl. Catal. B: Environ. 87 (2009) 105–145.

[7] M. Panizza and G. Cerisola, Direct and mediated anodic oxidation of organic pollutants, Chem. Rev. 109 (2009) 6541-6569.

[8] G. Chen, Electrochemical technologies in wastewater treatment, Sep. Purif. Technol. 38 (2004) 11-41.

[9] P. Cabot, J. Casado, E. Brillas, Electrochemical Methods for Degradation of Organic Pollutants in Aqueous Media, in M.A. Tarr (Ed.), Chemical Degradation Methods for Wastes and Pollutants: Environmental and industrial applications, CRC Press, 2003.

[10] K. Rajeshwar, J. Ibanez, Environmental Electrochemistry Fundamentals and Applications in Pollution Abatement, Academic Press Inc., San Diego, 1997.

[11] D. Simonsson, Electrochemistry for a cleaner environment, Chem. Soc. Rev. 26 (1997) 181-189.

[12] P.V. Nidheesh, R. Gandhimathi, Trends in electro-Fenton process for water and wastewater treatment: An overview, Desalination 299 (2012) 1-15.

[13] C.M. Sanchez-Sanchez, E. Expósito, J. Casado, V. Montiel, Goethite as a more effective iron dosage source for mineralization of organic pollutants by electro-Fenton process, Electrochem. Commun. 9 (2007) 19-24.

[14] E. Brillas, J. Casado, Aniline degradation by Electro-Fenton and peroxi-coagulation processes using a flow reactor for wastewater treatment, Chemosphere 47 (2002) 241-248.

[15] C.A. Martínez-Huitle, S. Ferro, Electrochemical oxidation of organic pollutants for the wastewater treatment: direct and indirect processes, Chem. Soc. Rev. 35 (2006) 1324–1340.

[16] J. Iniesta, E. Expósito, J. Gonzalez-Garcia, V. Montiel, A. Aldaz, Electrochemical treatment of industrial wastewater containing phenols, J. Electrochem. Soc. 149 (2002) D57-D62.

[17] M. Panizza, P.A. Michaud, G. Cerisola, C. Comninellis, Electrochemical treatment of wastewaters containing organic pollutants on boron-doped diamond electrodes: Prediction of specific energy consumption and required electrode area, Electrochem. Commun. 3 (2001) 336-339.

[18] F. Fu, Q. Wang, Removal of heavy metal ions from wastewaters: A review, J. Environ. Manag. 92 (2011) 407-418.

[19] P. Maha Lakshmi, P. Sivashanmugam, Treatment of oil tanning effluent by electrocoagulation: Influence of ultrasound and hybrid electrode on COD removal, Sep. Purif. Technol. 116 (2013) 378-384.

[20] D. Valero, J.M. Ortiz, V. García-García, E. Expósito, V. Montiel, A. Aldaz, Electrocoagulation of wastewater from almond industry, Chemosphere 84 (2011) 1290–1295.

[21] I. Linares-Hernández, C. Barrera-Díaz, B. Bilyeu, P. Juárez-GarcíaRojas, E. Campos-Medina, A combined electrocoagulation–electrooxidation treatment for industrial wastewater, J. Hazard. Mater. 175 (2010) 68-694.

[22] M.M. Emamjomeh, M. Sivakumar, Review of pollutants removed by electrocoagulation and electrocoagulation/flotation processes, J. Environ. Manag. 90 (2009) 1663-1679.

[23] D. Valero, J.M. Ortiz, E. Expósito, V. Montiel, A. Aldaz, Electrocoagulation of a synthetic textile effluent powered by photovoltaic energy without batteries: Direct connection behaviour, Sol. Energy Mater. Sol. Cells, 92 (2008) 291-297.

[24] EPSAR, Modelo de ordenanza de vertidos, web epsar.

[25] Ordenanza municipal de vertidos de Xixona, BOPA 220, 24/09/2001, 11-14.

[26] REAL DECRETO 1620/2007, de 7 de diciembre, por el que se establece el régimen jurídico de la reutilización de las aguas depuradas, BOE 294, 08/12/2007 50639-50661.

[27] Ch. Comninellis, A. Kapalka, S. Malato, S. A. Parsons, I. Poulios, D. Mantzavinos, Advanced oxidation processes for water treatment: advances and trends for R&D, J. Chem. Technol. Biotechnol. 83 (2008) 769–776.

[28] J. Iniesta, P.A. Michaud, M. Panizza, G. Cerisola, A. Aldaz, Ch. Comninellis, Electrochemical oxidation of phenol at boron-doped diamond electrode, Electrochim. Acta 46 (2001) 3573–3578.

[29] M. Deborde, U. von Gunten, Reactions of chlorine with inorganic and organic compounds during water treatment – Kinetics and mechanisms: A critical review, Wat. Res. 42 (2008) 13-51.

[30] J.G. March, M. Gual, Studies on chlorination of greywater, Desalination, 249 (2009) 317-322.

[31] S. Aquino Neto, A.R. de Andrade, Electrooxidation of glyphosate herbicide at different DSA compositions: pH, concentration and supporting electrolyte, Electrochim. Acta 54 (2008) 2039-2045.

[32] E. Alvarez-Guerra, A. Dominguez-Ramos, A. Irabien, Design of the Photovoltaic Solar Electro-Oxidation (PSEO) process for wastewater treatment, Chem. Eng. Res. Des. 89 (2011) 2679-2685.

[33] D. Valero, J. M. Ortiz, E. Expósito, V. Montiel, A. Aldaz, Electrochemical Wastewater Treatment Directly Powered by Photovoltaic Panels: Electrooxidation of a Dye-Containing Wastewater, Environ. Sci. Technol. 44 (2010) 5182–5187.

[34] J.M. Ortiz, E. Expósito, F. Gallud, V. Garcia-Garcia, V. Montiel, A. Aldaz, Desalination of underground brackish waters using an electrodialysis system powered directly by photovoltaic energy, Sol. Energy Mater. Sol. Cells 92 (2008) 1677-1688.

[35] J.M. Ortiz, E. Expósito, F. Gallud, V. García-García, V. Montiel, A. Aldaz, Electrodialysis of brackish water powered by photovoltaic energy without batteries: direct connection behaviour, Desalination 208 (2007) 89-100.

[36] T.U. Townsend, A method for estimating the long-term performance of direct-coupled photovoltaic systems, M.Sc. Thesis, Solar Energy Laboratory, University of Wisconsin, Madison, 1989, http://sel.me.wisc.edu/publications/theses/townsend89.zip .

[37] A. Kapalka, G. Fóti, C. Comninellis, Kinetic modelling of the electrochemical mineralization of organic pollutants for wastewater treatment, J. Appl. Electrochem. 38 (2008) 7-16.

[38] S. Trasatti, Electrocatalysis: understanding the success of DSA, Electrochim. Acta 45 (2000) 2377-2385.

[39] D. Gandini, E. Mahé, P.A. Michaud, W. Haenni, A. Perret, Ch. Comninellis, Oxidation of carboxylic acids at boron-doped diamond electrodes for wastewater treatment, J. Appl. Electrochem. 30 (2000) 1345-1350.

[40] A. M. Couper, D. Pletcher, F. C. Walsh, Electrode Materials for Electrosynthesis, Chem. Rev. 90 (1990) 837-865.

[41] M.R. Gonçalves, I.P. Marques, J.P. Correia, Electrochemical mineralization of anaerobically digested olive mill wastewater, Water Res. 46 (2012) 4217-4225.

[42] E. Chatzisymeon, A. Dimou, D. Mantzavinos, A. Katsaounis, Electrochemical oxidation of model compounds and olive mill wastewater over DSA electrodes: 1. The case of Ti/IrO_2 anode, J. Hazard. Mater. 167 (2009) 268-274.

[43] G.R.P. Malpass, D.W. Miwa, S.A.S. Machado, A.J. Motheo, Decolourisation of real textile waste using electrochemical techniques: Effect of electrode composition, J. Hazard. Mater. 156 (2008) 170-177.

[44] M.R.G. Santos, M.O.F. Goulart, J. Tonholo, C.L.P.S. Zanta, The application of electrochemical technology to the remediation of oily wastewater, Chemosphere 64 (2006) 393-399.

[45] A. Luque, S. Hegedus, Handbook of Photovoltaic science and engineering, John Wiley & Sons, West Sussex, 2003.

HIGHLIGHTS

- Electrooxidation was applied to real wastewater from an almond industry.
- Best conditions for treatment were determined and scaled to pre-industrial.
- Electrooxidation at pre-industrial scale is an effective technology for this water.
- Contaminants were removed from industrial wastewater in a high extension.
- Economic parameters and costs were calculated.